KSME

Springer

Journal of Mechanical Science and Technology 34 (2) 2020

Original Article
DOI 10.1007/s12206-020-0107-6

Keywords:
· Face gear
· Split-torque transmission system
· Mesh stiffness
· Semi-analytical method
· Time-varying

Correspondence to:
Jinyuan Tang
jytangcsu_312@163.com
Yi Wang
djx_ylmj@163.com

Citation:
Dong, J., Tang, J., Hu, Z., Wang, Y. (2020). A semi-analytical method of time-varying mesh stiffness in concentric face gear split-torque transmission system. Journal of Mechanical Science and Technology 34 (2) (2020) 589~602. http://doi.org/10.1007/s12206-020-0107-6

Received July 18th, 2019
Revised November 10th, 2019
Accepted December13th, 2019

† Recommended by Editor No-cheol Park

A semi-analytical method of time-varying mesh stiffness in concentric face gear split-torque transmission system

Jianxiong Dong[1,2], Jinyuan Tang[2,3], Zehua Hu[2,3] and Yi Wang[4]

[1]Light Alloy Research Institute, Central South University, Changsha 410083, China, [2]State Key Laboratory of High Performance Complex Manufacturing, Central South University, Changsha 410083, China, [3]School of Mechanical and Electrical Engineering, Central South University, Changsha 410083, China, [4]School of Aeronautics and Astronautics, Central South University, Changsha 410083, China

Abstract Concentric face gear split-torque transmission system (CFGSTTS) has great applied value in the field of aeronautical transmission due to the characteristic of high integration. Mesh stiffness, as one of the most primary sources of vibration, is vitally important for the dynamic performances of gear transmission system. The existing finite element method (FEM) and analytical method (AM) are not suitable for tackling the mesh stiffness calculation of closed-loop multi-branch system such as CFGSTTS. Thus, a semi-analytical method (SAM) is presented and verified, which combines the high precision of FEM with the high efficiency of AM. Additionally, the differences between the mesh stiffness of independent face gear drive and that of the same gear pair in CFGSTTS under accordant load is researched by applying SAM. The influence rules of distribution angle and load condition on the mesh stiffness of gear pairs considering system structure are also studied. Results demonstrate that the mesh stiffness of gear pairs in CFGSTTS is time-varying and tends to be consistent with each other by adjusting load parameters.

1. Introduction

Concentric face gear split-torque transmission system (CFGSTTS) has advantages of high power density, compact structure and no axial force, which makes it a new trend of application in high-speed, heavy-load transmission system. As is known to all, time-varying mesh stiffness (TVMS) is one of the most important sources of vibration and noise, and the premise of studying dynamic characteristics of gear system. Therefore, the research of mesh stiffness of a complex system such as CFGSTTS is essential for the optimization of structure and performance.

Previous researches about gear stiffness mainly focus on cylindrical gears. The main calculation methods include analytical method (AM), finite element method (FEM) and some other methods derived from these two methods. Marques et al. [1] established an analytical model of mesh stiffness based on Heaviside functions, and proposed a concept of gear design with constant stiffness. Cooley et al. [2] compared the average slope method with the local slope method for mesh stiffness calculation and concluded that the former is suitable to static analysis while the latter should be used for dynamic analysis. Guo et al. [3] studied the mesh stiffness of gear pairs in back-side contact which occurs as teeth separate and pass the backlash zone. Xie et al. [4] delved into an improved calculation method of mesh stiffness with considering the structure coupling effect. Pedersen et al. [5] presented a method to estimate the stiffness of individual gear tooth at the position of contact point by using FE analysis and found that rim thickness and load size must be considered for stiffness estimating. Chang et al. [6-8] employed an integrated approach to calculate mesh stiffness considering the linear global deformation and nonlinear local deformation. All these studies are based on spur gears, and all considered variables turn out to have influence on mesh stiffness. These calculation methods for mesh stiffness was proved to be correct by comparing with the results of ISO standard or FEM.

As is known to all, the mesh stiffness of helical gear is slightly more complicated than that of spur gear. Wang et al. [9] focused on an improved TVMS model of helical gears. In their stiffness model, the transverse and axial parameters such as bending, shear, compressive stiffness, foundation stiffness and Hertzian contact were considered.

Generally, the mesh stiffness of other gear forms besides cylindrical gear such as bevel gear and planetary gear cannot be calculated by AM, but by FEM. Sheveleva et al. [10] defined a mesh algorithm based on grid presentation for analyzing spiral bevel gear, and programmed the computer codes which contain transmission errors, contact paths, contact areas and contact pressure distributions. Medvedev et al. [11] constructed an algorithm to define the torque transmitted by each gear pair in multi-tooth contact of spiral bevel gear. This algorithm can automatically detect the contact tooth logarithm, which is universal and can be used to study the multi-pair contact problems of arbitrary gears.

In fact, gear mesh stiffness can be affected by external factors including friction and lubrication. Rincon et al. [12] described an analysis model for mesh stiffness of spur gear with friction. Their stiffness model considered the global and local deformation which is calculated by FEM and AM respectively. Saxena et al. [13] conducted a computer simulation to study the effect of time-varying friction coefficient on the total effective mesh stiffness of spur gear.

Above studies are based on healthy teeth. However, the effects of cracks, pitting corrosion, spalling and other gear defects on mesh stiffness have gradually attracted researchers' attention. Cui et al. [14-17] devoted to the mesh-stiffness calculation of cracked gears based on the universal equation of gear profile and revealed that mesh stiffness decreases as the depth of crack increases, which enables a good prediction on the mesh stiffness for a spur gear pair with both incipient and larger tooth cracks. Luo et al. [18, 19] shared a shape-independent method to model tooth spalling based on defect ratios instead of a specific geometry to calculate mesh stiffness of gears with crack. Their results indicate that the TVMS of healthy gear or gear under conditions with various tooth spalling can be predicted. Ma et al. [20, 21] gave new analysis models for the TVMS calculation of cracked spur gears, and the influence of long tooth contact on transient moment as well as gear mesh stiffness on vibration were considered.

The test of gear mesh stiffness is the verification of theoretical methods and covers the influence of all factors comprehensively. Raghuwanshi et al. [22] contributed a new experimental technique of mesh stiffness measurement by using digital image correlation (DIC) technique to measure healthy and cracked gears. Compared to the results of DIC, the magnitude of mesh stiffness has been observed slightly higher in results of FEM and AM.

However, the existing researches about gear stiffness do not take system structure into account, and the stiffness investigation of closed-loop system composed of face gears is rarely involved. Compared with the mesh stiffness of open-loop gear chain or independent gear drive, the mesh stiffness of gear pair in closed-loop system embodies difference and particularity. In this paper, the structural characteristics of CFGSTTS are introduced first. And then, the mechanism characteristics of CFGSTTS are analyzed from the aspects of degree of freedom (DOF), deterministic motion condition and TVMS. Furthermore, a semi-analytical method (SAM) for calculating TVMS of gear pairs considering system structure is proposed and verified by being compared with the stiffness formula of spur gear in ISO. The innovations of SAM lie in the development of a new finite element model for closed-loop gear system as well as the accurate calculation of time-varying moment arm and the analytical algorithm for the stiffness of multi-tooth meshing. In addition, the characteristics of TVMS of gear pairs in CFGSTTS and the influence of system parameters on TVMS are explored by using SAM.

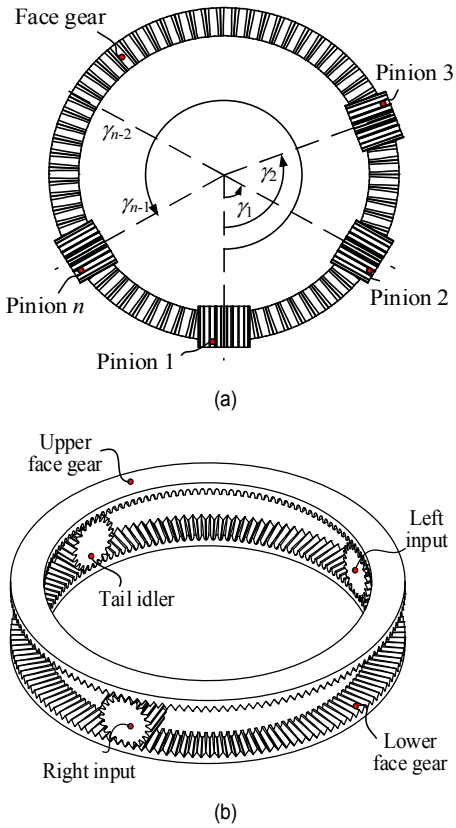

Fig. 1. Structure of CFGSTTS: (a) Top view; (b) isometric view for the system with three pinions.

2. Concentric face gear split-torque transmission system

The structure of CFGSTTS is demonstrated in Fig. 1. Two face gears are oppositely mounted on one axis and multiple pinions are distributed on the circumference of face gears. As shown in Fig. 1(a), once an axis of pinion is selected as reference, the position of other pinions is determined by angle γ_i (i = 1,2...n-1) which is called distribution angle [23]. The axes of

all pinions intersect the axes of face gears at one point. Moreover, each pinion simultaneously meshes with the upper and lower face gears.

Generally, CFGSTTS serves as a multi-input and multi-output transmission with multiple power branches, and its advantages are mainly reflected in following aspects:

(a) Multiple input gears which connected to engines provide great power to the system. In the event of a single-engine failure, power can still be obtained from unbroken input terminals, and at this moment the system can be switched into a low-power mode and work continuously.

(b) Multiple output terminals can meet the power demand of multiple parts in a mechanical system, reducing the number of power devices.

(c) Concentric structure makes the system more compact and shrinks the whole size.

(d) The power capacity of the system can be further expanded by adding pinions.

As to a face gear drive, whether the pinion is straight or helical, cylindrical or conical, it can be assembled into a CFGSTTS. This study mainly focuses on three-pinion CFGSTTSs. The pinions are orthogonal spur gears with involute profile, as presented in Fig. 1(b). Two pinions act as input terminals named as left input and right input. The other pinion is output terminal named as tail idler. The main power of the system is output from upper face gear and a small amount is transmitted from tail idler.

From the perspective of mechanism theory, the prerequisite for a mechanical structure to achieve deterministic motion is that the number of driving elements is equal to DOF. Provided that only one pinion exists, the system in Fig. 1(b) can be normally operated. As two input gears are rotating synchronously without phase difference, they can be replaced by one input pinion. Tail idler does not affect DOF, so it can be deleted. The simplified CFGSTTS has only one driving element and its DOF is 1. Therefore, the system has deterministic motion. As several virtual constraints exist, CFGSTTS in Fig. 1(b) is a statically indeterminate structure. Another feature of CFGSTTS is that closed loops can be formed by power branches, that is, two pinions and two face gears can form into a closed loop end to end. TVMS is another outstanding feature of CFGSTTS. Research shows that load condition has a great impact on mesh stiffness [5]. The loads of gear pairs in CFGSTTS are very likely to be different, which indicates the diversity of mesh stiffness among different gear pairs. In addition, the asymmetry of power branches is also an important point to distinguishes CFGSTTS from ordinary split-torque transmission system, which is mainly reflected that the number of gear pairs and the form of structural parts in different power branches are inconsistent.

3. Model and validation

3.1 Semi-analytical method

The main idea of SAM is to calculate the force and coordinate of the contact point with a new finite element model and transmission error (TE) by AM, then the mesh stiffness can be obtained.

The calculation of TVMS for gear pairs in CFGSTTS is based on the following hypotheses:

(i) Since mesh stiffness reflects the material property and characteristics of contact surfaces, only the deformation of gear teeth is considered with ignoring the deformation of hubs and other structures.

(ii) Gear pairs have no clearance that is caused by geometric errors and installation errors.

3.1.1 A new finite element model

In the analysis of a complex gear system with closed loops and multiple branches, convergent results cannot be obtained by existing finite element model [24-27] due to insufficient refinements of boundary conditions, step setting et al. In order to simulate closed-loop gear systems, a new finite element model has been developed. The innovations are represented as follows:

(i) Several steps which are not arranged in existing model are set up artificially to control the simulation process of CFGSTTS.

Step 1: Six DOFs of each gear are constrained.

Step 2: Face gears rotate by a tiny angle of φ_1 in the opposite direction of their actual rotation around their axes respectively to contact with two input gears. Meanwhile, tail idler rotates by a tiny angle of φ_2 in the opposite direction of actual rotation to contact with two face gears. It is worth noting that these two reverse angles need to satisfy the relation:

$$\varphi_2 > \varphi_1 \times \frac{Z_g}{Z_p} \tag{1}$$

where Z_p is the tooth number of a driving gear, and Z_g is the tooth number of a driven gear. In a face gear drive, the face gear is drove by the pinion.

Step 3: The rotational constraints around axes are released, and two small loads are applied to power output terminals respectively, namely upper gear and tail idler.

Step 4: The actual loads are applied to tail idler and upper face gear, and an accordant rotation angle are added to two input gears.

(ii) Before boundary conditions are defined, gears in CFGSTTS are divided into three categories. Two input pinions act as the first type. Two face gears belong to the second type, and tail idler is the third type. In the establishment of contact pairs in which the driving and driven gear is not determined, the entire tooth groove and tooth profile that may be in contact are defined as contact surfaces, as presented in Fig. 2. By doing this, the mechanical information of both front-side contact and back-side contact can be output. Whereas, the existing finite element model only defines one side of gear tooth as contact surface.

Generally, the choice of master and slave surfaces is based on following considerations: (a) The surfaces of output gears

Table 1. Boundary conditions in new finite element model.

Steps	Face gears	Input gears	Tail idler
Initial	Fixed	Fixed	Fixed
1	Slight rotate in reverse	Fixed	Slight rotate in reverse
2	Free	Fixed	Free
3	Free	Fixed	Free
4	Free	Rotate	Free

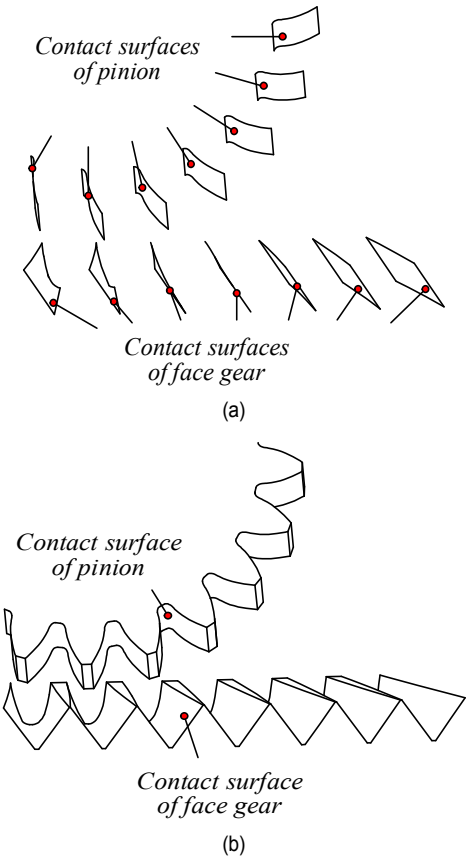

Fig. 2. Contact surfaces: (a) Existing model; (b) new model.

are taken as slave surfaces while output gears are meshing with other gears. (b) The surfaces of input gears are treated as master surfaces when input gears are contacting with others. (c) As to gear pairs which are formed by neither input nor output gears, surfaces on pinions are recommended as master surfaces.

(iii) The boundary condition in Table 1 are designed specifically for closed-loop gear systems, which is more complicated than that in existing finite element model.

3.1.2 Analytical algorithm

The coordinates of contact point and contact force of gear pairs in global coordinate system can be directly extracted from simulation results.

In the stiffness calculation of spur gears, moment arm is often regarded as a constant value and replaced by the radius of base circle. CFGSTTS is mostly applied in conditions of heavy load, thus, big modulus is used and correspondingly results in large size of gear body. In order to reduce theoretical errors, the precise calculation of time-varying moment arm become essential for mesh stiffness calculation.

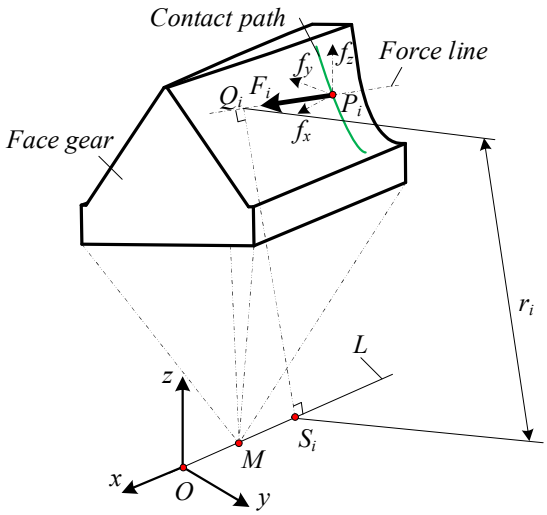

Fig. 3. Diagram of moment arm.

As reflected in Fig. 3, in a single-tooth meshing period, the contact path on the surface of face gear is composed of contact points whose coordinates are $P_i(x_i, y_i, z_i)$. Contact force F_i acts on contact point P_i and is projected on each coordinate axis, namely, the component forces are f_x, f_y and f_z respectively. Line L is the spin axis of face gear. Q_i is another point on the extension line of contact force F_i. The point Q_i and point S_i are on the common perpendicular between line L and the extension line of contact force F_i. Face gear is constrained to point M on its axis.

According to the theory of spatial geometry, the direction vector of line L in global coordinate system [O; x, y, z] is:

$$\vec{n_l} = (1, 0, 0) \tag{2}$$

The direction vector of the extension line of contact force at point P_i is:

$$\vec{n_p} = (f_x, f_y, f_z) \tag{3}$$

The direction vector of the common perpendicular between line L and the extension line of contact force can be expressed as:

$$\vec{n} = \vec{n_p} \times \vec{n_l} \tag{4}$$

Point O is on line L, and point P_i is on the extension line of contact force. These two points can compose a vector:

$$\overrightarrow{OP_i} = (x_i, y_i, z_i) \tag{5}$$

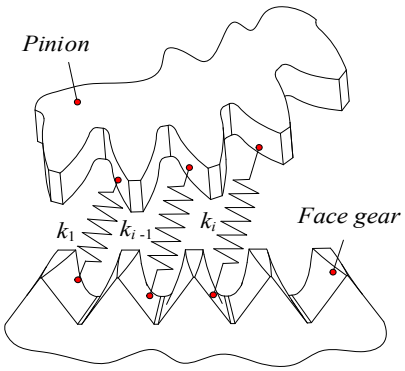

Fig. 4. Mesh stiffness model of multi-tooth area.

The projection of the vector of Eq. (5) in the direction of common perpendicular of Eq. (4) is the vertical distance of space. Therefore, time-varying moment arm is

$$r_i = \left|\overrightarrow{S_iQ_i}\right| = \frac{\overrightarrow{OP_i}\cdot\vec{n}}{\left|\vec{n}\right|} \tag{6}$$

The coordinate values of vector are substituted, and Eq. (6) can be simplified as:

$$r_i = \frac{f_y\cdot z_i - f_z\cdot y_i}{\sqrt{f_y^2+f_z^2}} \tag{7}$$

Generally, the TE of a gear pair [28] is:

$$e = \theta_g - \frac{Z_p}{Z_g}\cdot\theta_p \tag{8}$$

where θ_p and θ_g are the rotation angles of pinion and face gear respectively under actual load condition. In practice, the geometrical model may have tooth surface errors including machining errors, assembly errors and meshing errors. In order to eliminate the influence of those errors, the no-load TE is usually required to be subtracted in deformation calculations. To be specific, the clearance caused by errors can be eliminated in finite element simulation with a small load closed to 0, and no-load TE can be solved and expressed as:

$$e_n = \theta_{ng} - \frac{Z_p}{Z_g}\cdot\theta_{np} \tag{9}$$

where θ_{np} and θ_{ng} are the rotation angles of pinion and face gear respectively under a small load.

The gear deformation can be calculated according to time-varying moment arm and TE.

$$\delta_i = r_i\cdot(e-e_n) \tag{10}$$

In actual working conditions, it is possible for a gear pair to be meshed with multiple teeth simultaneously, which will result in the meshing alternation of single tooth and multiple teeth. In studying the relationship between the force and deformation of single teeth-meshing area, a tooth pair can be simplified as a spring [4, 9]. The mesh stiffness of a tooth pair can be presented by the following formula.

$$k_i = \frac{F_i}{\delta_i} \tag{11}$$

In multiple teeth-meshing area, tooth pairs can be equivalent to a system with multiple springs, as shown in Fig. 4. The mesh stiffness of a gear pair can be also expressed as the ratio of the total force and the amount of deformation. The acting force can be obtained by dividing the torque of the gear pair by an equivalent moment arm. The deformation of a gear pair can be expressed as the product of the equivalent moment arm and the actual transmission error.

Based on the moment distribution of each tooth pair in multiple tooth-meshing area, the equivalent moment arm can be represented as

$$\bar{r} = \sum_i^n r_i\frac{F_ir_i}{\sum_j^n F_jr_j} \tag{12}$$

According to the deformation relation, when multiple teeth are in contact simultaneously, the energy consumed by overall deformation is the sum of the energy consumed by deformation of meshed teeth. Thus, the calculation of comprehensive mesh stiffness in multiple teeth-meshing area is something like that of multiple springs in parallel. The comprehensive mesh stiffness in multiple teeth-meshing area is simplified as:

$$K = \frac{\sum_i^n F_ir_i}{\bar{r}^2\cdot(e-e_n)} \tag{13}$$

where *i* is the number of engaged teeth. The above formulas of time-varying moment arm, torque and mesh stiffness can be programmed into codes to improve computing efficiency and avoid repetitive work.

3.2 Validation

According to ISO 6336 [29], if the load of tooth per unit width is larger than 100 N/mm, the maximum stiffness of tooth per unit width in single teeth-meshing area is:

$$c' = \frac{C_MC_RC_B}{0.04723+\frac{0.15551}{Z_p}+\frac{0.25791}{Z_g}} \tag{14}$$

where C_M is the correction factor, C_R is the gear blank factor,

and C_B is the basic rack factor.

If contact ratio ε is larger than 1.2, the mean value of mesh stiffness per unit width in multiple teeth-meshing area can be represented as [29]:

$$c_{\gamma\alpha} = (0.75 * \varepsilon + 0.25) \cdot c' \tag{15}$$

Here, the formula of no-load contact ratio [29] of involute spur gear is

$$\varepsilon = \frac{Z_p\left(\tan\alpha_{ap} - \tan\alpha\right) + Z_g\left(\tan\alpha_{ag} - \tan\alpha\right)}{2\pi} \tag{16}$$

where α_{ap} and α_{ag} are the pressure angle at the tooth top of driving and driven gear [29], respectively.

$$\alpha_{ai} = \arccos\left(\frac{R_i \cos\alpha}{R_{ai}}\right) \quad i = p, g \tag{17}$$

Here, R_i and R_{ai} are the reference radius and outside radius respectively.

Since the contact ratio in gear drives is greatly affected by the load, the mesh stiffness should be calculated with loaded contact ratio. The method of calculating mesh stiffness with loaded contact ratio can be counted as improved ISO.

Contact ratios [28] can be expressed as:

$$\varepsilon = \frac{\Delta\theta_1}{2\pi} \times Z_p \tag{18}$$

where $\Delta\theta_1$ is the rotation angle of pinion during the meshing period of a single tooth. The ratio of 2π to Z_p is equal to the rotation angle of pinion during the period when two adjacent teeth are engaged in succession. On the condition of uniform rotation, contact ratios in Eq. (18) can also be formulated as:

$$\varepsilon_L = \frac{\Delta T}{\Delta t} \tag{19}$$

where ΔT is the duration of a tooth from engagement to withdrawal. Δt is the time difference of adjacent teeth entering meshing one after another.

The spur gear drive with parameters in Table 2 is applied for the validation of SAM, and the contact forces calculated with the new finite element model are presented in Fig. 5(a). Integrating above introductions, the comparison results of mesh stiffness calculated by three methods including SAM, ISO and improved ISO are demonstrated in Fig. 5(b).

Based on Eqs. (16) and (17), it can be calculated that the no-load contact ratio of the involute spur gear drive in Table 2 is 1.4. Results in Fig. 5(a) demonstrate that ΔT is equal to 0.224, and Δt is 0.14. Thus, the loaded contact ratio turns out to be 1.6 based on the Eq. (19). This indicates that there is a big difference between loaded contact ratio and no-load one,

Table 2. Parameters of spur gear drive.

Parameters	Numerical values
Modulus m (mm)	4
Pressure angle α (°)	25
Tooth number of driving gear Z_p	25
Tooth number of driven gear Z_g	33
Tooth width B (mm)	28
Young's modulus E (GPa)	209
Poisson's ratio v	0.29
Load torque T (N.m)	660

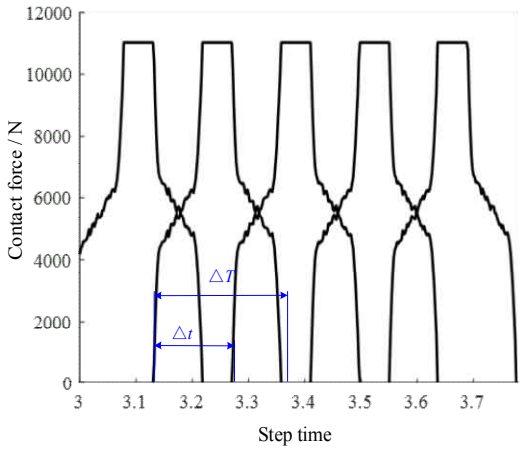

(a)

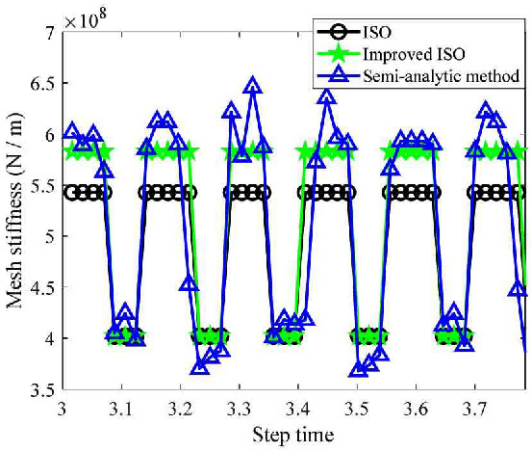

(b)

Fig. 5. Comparison of three methods: (a) Contact force; (b) mesh stiffness.

which greatly influences mesh stiffness calculating. In the diagram of contact forces (see Fig. 5(a)), an alternation of double tooth meshing and single tooth meshing has occurred.

Fig. 5(b) reveals that the meshing phase of TVMS calculated by three methods is completely consistent both in single tooth meshing and double tooth meshing. In single teeth-meshing area, the stiffness calculated by three methods is basically the same. Nevertheless, in double teeth-meshing area, only the

Table 3. Parameters of face gear drives.

Parameters	Numerical values
Modulus (mm)	4
Pressure angle (°)	20
Tooth number of spur gear Z_p	21
Tooth number of face gear Z_g	142
Inner radius of face gear (mm)	270
Outer radius of face gear (mm)	325
Tooth width of face gear (mm)	55
Tooth width of spur gear (mm)	60

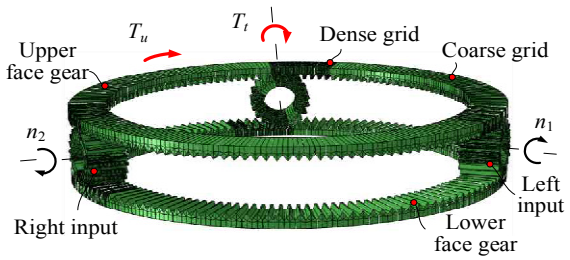

Fig. 6. Finite element model.

stiffness calculated by improved ISO, namely the method with loaded contact ratio is basically consistent with that by SAM, and the relative error of those two methods is 2.8 %. Specifically, the mesh stiffness calculated by improved ISO is slightly less than that by SAM. The reason is that ISO algorithm calculates average stiffness in multiple teeth-meshing area, while SAM aims at calculating the actual mesh stiffness. The obvious difference between mesh stiffness of no-load contact ratio (ISO) and that of loaded contact ratio (improved ISO) is only reflected in double teeth-meshing area, and the relative error is within 7.4 %.

In conclusion, mesh stiffness calculated by SAM proposed in this study is credible whose results are more consistent with the results of improved ISO.

4. Numerical examples and discussions

The geometric parameters of face gears in all examples in this paper are consistent with Table 3.

4.1 Numerical example 1

The structure of CFGSTTS is shown in Fig. 1(b) and the distribution angles are 110.282° and 249.718°. The established finite element model is shown in Fig. 6.

The whole model contains 284330 grids and 394132 nodes. Eight teeth in the contact area of a gear are divided into dense grids, and the remaining teeth are coarse grids. The area near the contact surface of teeth is divided into dense grids and the other parts are coarse grids. These simplifications are helpful to improve the calculating accuracy and efficiency of the finite element model. All gears are steel with the properties of E = 2.068×10^5 N/mm^2 and Poisson's ratio v = 0.3. The torque T_t applied to the tail idler is 490 N·m, and the torque of T_u (10500 N·m) is loaded to upper face gear. In order to obtain enough calculating data, the simulation step is set as short as possible.

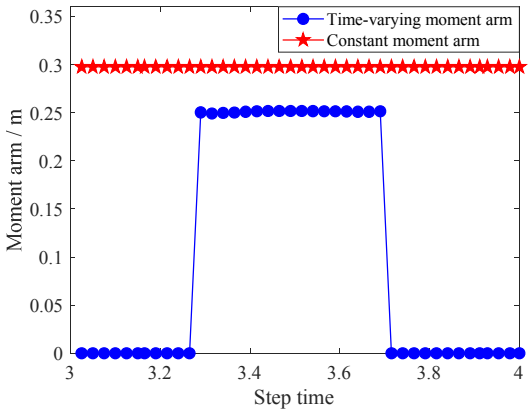

Fig. 7. Moment arms.

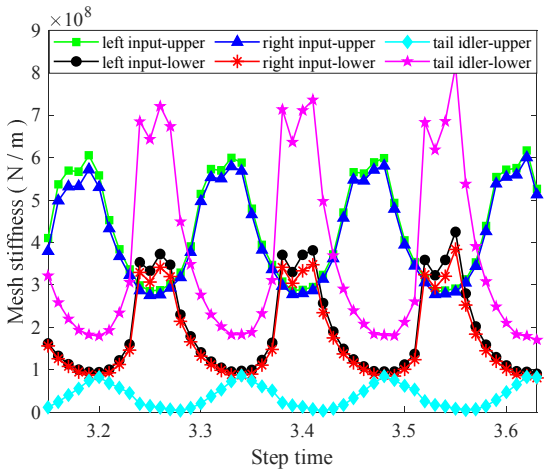

Fig. 8. Mesh stiffness of gear pairs in CFGSTTS.

The average of the inner radius and the outer radius of a face gear is generally treated as the constant moment arm of a driven gear. In the simulation results, the real-time moment arm of the gear pair composed of left input and upper face gear can be extracted. The comparison of constant moment arm and time-varying moment arm is demonstrated in Fig. 7.

According to the results in Fig. 7, when the single tooth of face gear is not engaged, the moment arm is 0. If engaged, the real-time moment arm is about 0.2515 m. However, the average of the inner radius and the outer radius of the face gear is 0.2975 m. Thus, the relate error of the constant moment arm and the time-varying moment arm is about 18.3 %, which is obvious and cannot be ignored.

In a CFGSTTS, three pinions and two face gears constitute six gear pairs. For convenience, the gear pair consisting of gear 1 and gear 2 is named as "gear 1-gear 2".

The time-varying mesh stiffness of gear pairs in CFGSTTS

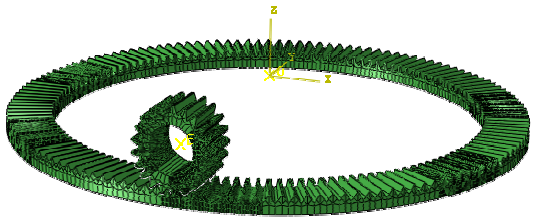

Fig. 9. Finite element model of face gear pair.

(see Fig. 8) can be obtained by SAM, and some conclusions can be drawn from the results in Fig. 8.

(i) The mesh stiffness curves of gear pairs in CFGSTTS are all periodic fluctuations, which is caused by the alternation of single tooth meshing and multiple tooth meshing. There are differences in stiffness curves which are mainly reflected in value and phase. Those differences are an important reason for vibration and noise.

(ii) Two input gears form two gear pairs by meshing with upper face gear, and the mesh stiffness of the gear pairs basically coincides. Likewise, as for the gear pairs consist of two input gears meshing with lower face gear, the mesh stiffness is also in accordance. Those consistency is determined by the positional symmetry of left and right input gears with respect to the axis of tail idler.

(iii) As for input gears, the mesh stiffness of the gear pairs formed by upper face gear is greater than that formed by lower face gear. Whereas, it is an opposite situation for tail idler.

(iv) When step time arrives to 3.2, all mesh stiffness curves of the gear pairs meshing with upper face gear reach peak value. While all mesh stiffness curves of the gear pairs meshing with lower face gear reach trough value. Consequently, for a same pinion gear, the mesh stiffness of the gear pairs which are composed by meshing with upper and lower face gears is not only significantly different in value, but also in phase difference of constant. Furthermore, the value difference of stiffness is result from the different load stressed by upper and lower face gear, and the odd teeth number of pinions result in the phase difference of stiffness. Similarly, the mesh stiffness curves of different pinions engaged with a same face gear may also have phase difference, which is related to the shaft angle between two pinions.

In order to explore the influence of closed-loop structure on mesh stiffness, the mesh stiffness of single pair of face gear drive are compared with that of gear pair in CFGSTTS. The gear pair "left input-upper" is taken as an example. The finite element model of face gear drive is demonstrated in Fig. 9, and it will be stressed by the torque (see Fig. 10) which loaded on the same gear pair in CFGSTTS. The model of face gear in Fig. 10 is simplified from the finite element model in Fig. 6.

The mesh stiffness of face gear drive can be obtained by SAM. The comparative diagram is demonstrated in Fig. 11.

The results show that the average mesh stiffness of face gear drive is about 1.45×10^8 N/m. When the gear pair bears the same load in CFGSTTS, the average mesh stiffness is nearly 4.50×10^8 N/m. Thus, mesh stiffness is not only related to load, but also to the structure of gear system. Due to the complexity of CFGSTTS, the mesh stiffness of each gear pair is likely to change with structural parameters. Therefore, it is necessary to study the variation rules of mesh stiffness of gear pairs considering system structure.

Table 4. Distribution angles.

Distribution angles	γ_1 (°)	γ_2 (°)
No.1	90	270
No.2	110.282	249.718
No.3	128.028	231.972
No.4	145.775	214.225
No.5	145.775	90

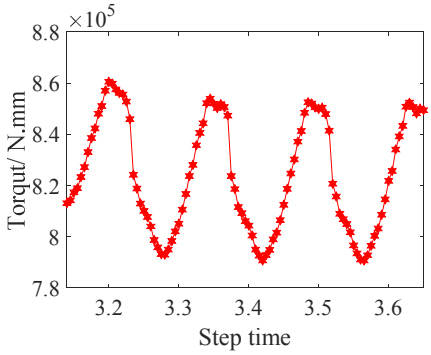

Fig. 10. Moment of gear pair "left input-upper".

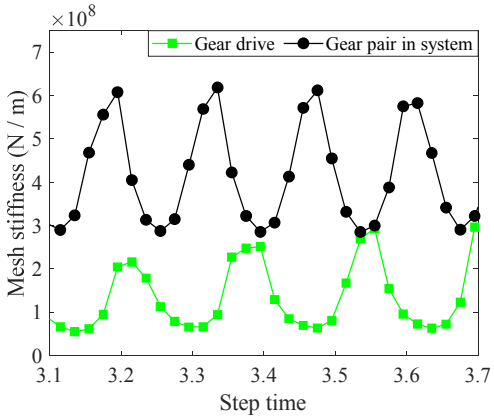

Fig. 11. Comparison of mesh stiffness.

4.2 Effect of system parameters on TVMS

In a CFGSTTS, all pinions rotate at a same speed, which is the same situation as face gears. Thus, the better the consistency and flatness of the mesh stiffness of gear pairs, the better the vibration performance of the system [1, 19]. The goal of researching mesh stiffness is to achieve its consistency.

Examples in this part are based on the finite element model in Fig. 6, and the materials of gear are consistent with that in

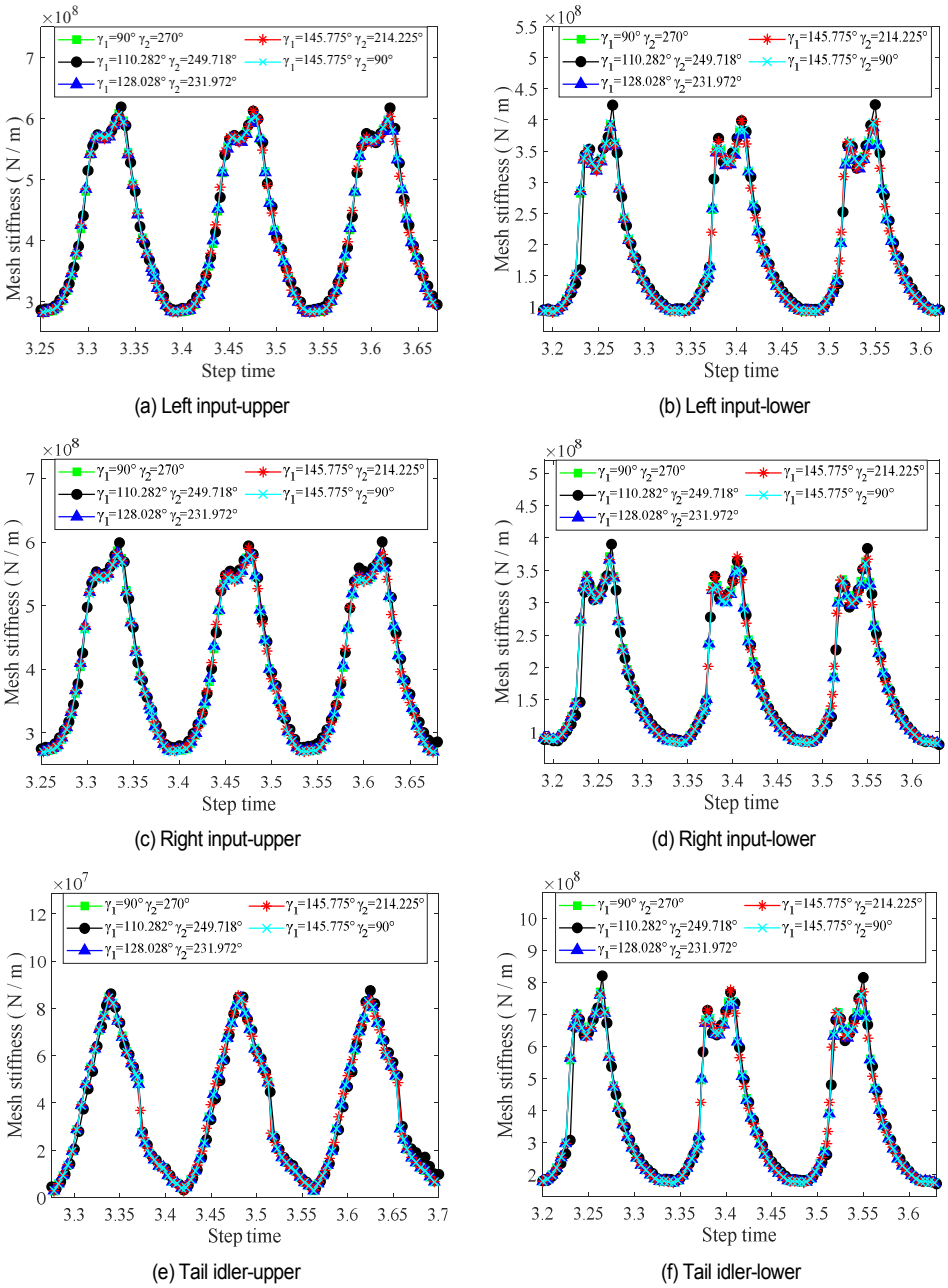

Fig. 12. TVMS in CFGSTTS with different distribution angles.

numerical example 1.

4.2.1 Distribution angle

As demonstrated in Fig. 1(b), tail idler is regarded as pinion 1 and take its axis as the reference. On this condition, the positions of left and right inputs can be expressed as angle γ_1 and γ_2.

Obviously, if two distribution angles add up to 360°, the positions of left and right inputs are symmetrical with respect to the axis of tail idler. The structure corresponding to different parameters of distribution angles in Table 4 is used for comparative analysis. In order to guarantee the single variable principle, all examples take the same load as numerical example 1.

Comparative results of TVMS of gear pairs in CFGSTTS with different distribution angles are calculated with SAM, as expressed in Fig. 12.

Among five groups of distribution angles, the left and right inputs of the previous four groups are symmetrical with the axis of tail idler, but the fifth group is asymmetric. As can be seen from the results in Fig. 12, the mesh stiffness of gear pairs in CFGSTTS with different distribution angles basically coincides. That is, the distributional position of pinions in the circumferential direction of face gears has no obvious influence on mesh stiffness, which is concluded on the premise that the flexibility

of shafts, hubs and some other structural parts is not considered. Since the characteristics of mesh stiffness have been specifically discussed in numerical example 1 and will not be described here.

Table 5. Load conditions.

Load torques	T_u (N/m)	T_t (N/m)
No.1	1500	70
No.2	6000	280
No.3	10500	490
No.4	15000	700
No.5	20996	1027

4.2.2 Load condition

In order to study the impact of load on the mesh stiffness of gear pairs in CFGSTTS, the same finite element model is taken for comparative study. The angle γ_1 and γ_2 are equal to 110.282° and 249.718° (see Fig. 1), respectively.

Symbol T_u represents the load torque of upper face gear, and the load torque of tail idler is reflected by the symbol T_t. Firstly, the load of upper face gear and tail idler is controlled to increase or decrease synchronously in proportion to study the

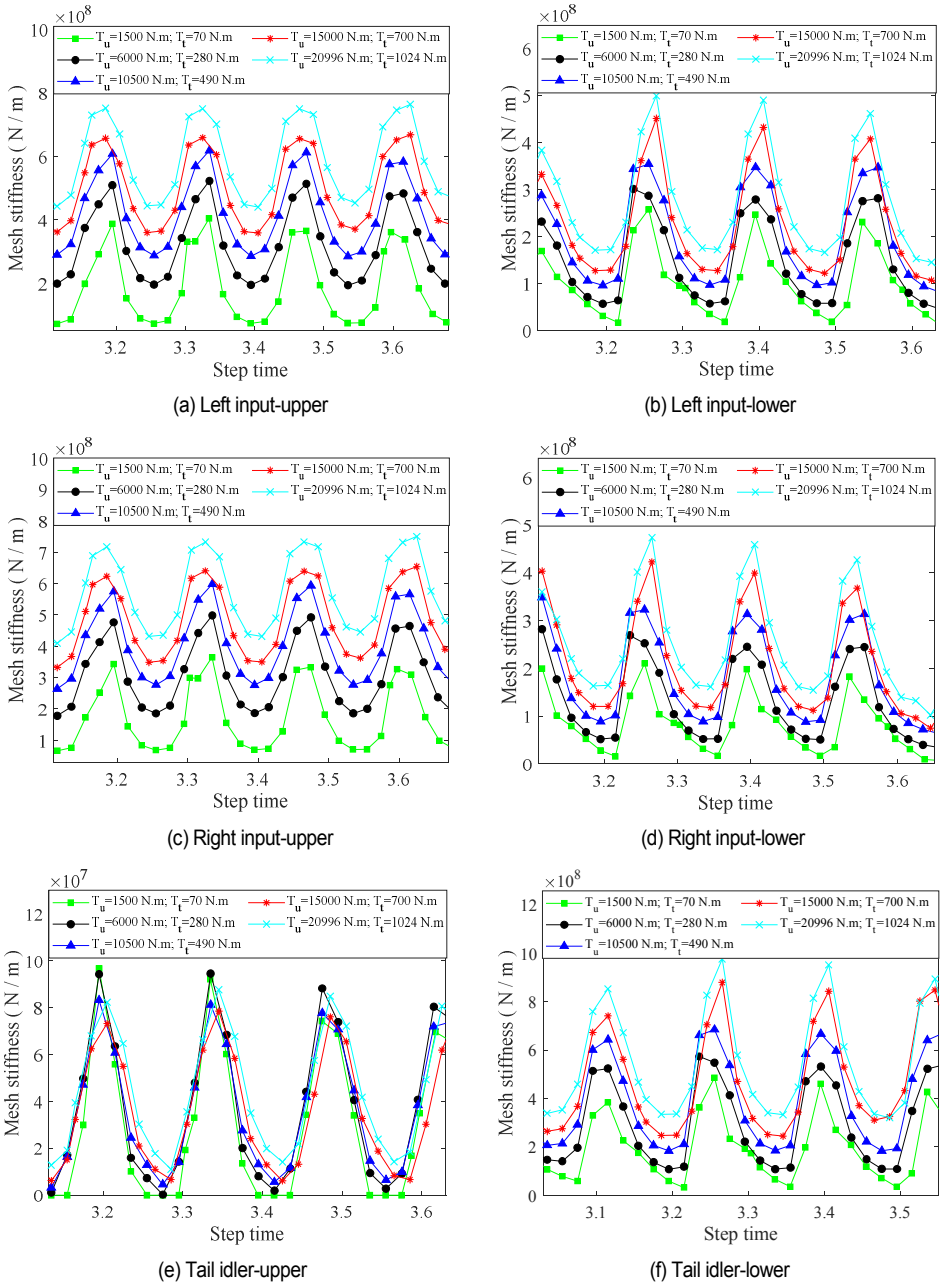

(a) Left input-upper (b) Left input-lower

(c) Right input-upper (d) Right input-lower

(e) Tail idler-upper (f) Tail idler-lower

Fig. 13. TVMS in CFGSTTS with different load torques.

changing trend of mesh stiffness. Different load torques in Table 5 are adopted for comparison.

Table 6. Parameters of load distribution.

Load	P_u (KW)	T_u (N/m)	P_t (KW)	T_t (N/m)	P (KW)
No.1	1500	12700	130	170	1630
No.2	1370	11600	260	330	1630
No.3	1240	10500	390	490	1630
No.4	1110	9400	520	650	1630
No.5	980	8300	650	810	1630

After calculation, the comparative results of mesh stiffness under different load conditions are presented in Fig. 13.

In general, the overall increase or decrease of the load on upper face gear and tail idler obviously affect mesh stiffness, as can be drawn from Fig. 10. As the load on upper face gear reaches the minimum value of 1500 N.m, the maximum values of the mesh stiffness of gear pairs are respectively equal to 3.9×10^8 N/m, 2.7×10^8 N/m, 3.5×10^8 N/m, 2.2×10^8 N/m, 0.9×10^8 N/m and 4.0×10^8 N/m. Nevertheless, when the load on upper face gear turns to the maximum value of 20996 N.m, the maximum values of the mesh stiffness of gear pairs are respectively equal to 7.5×10^8 N/m, 5×10^8 N/m, 7.3×10^8 N/m,

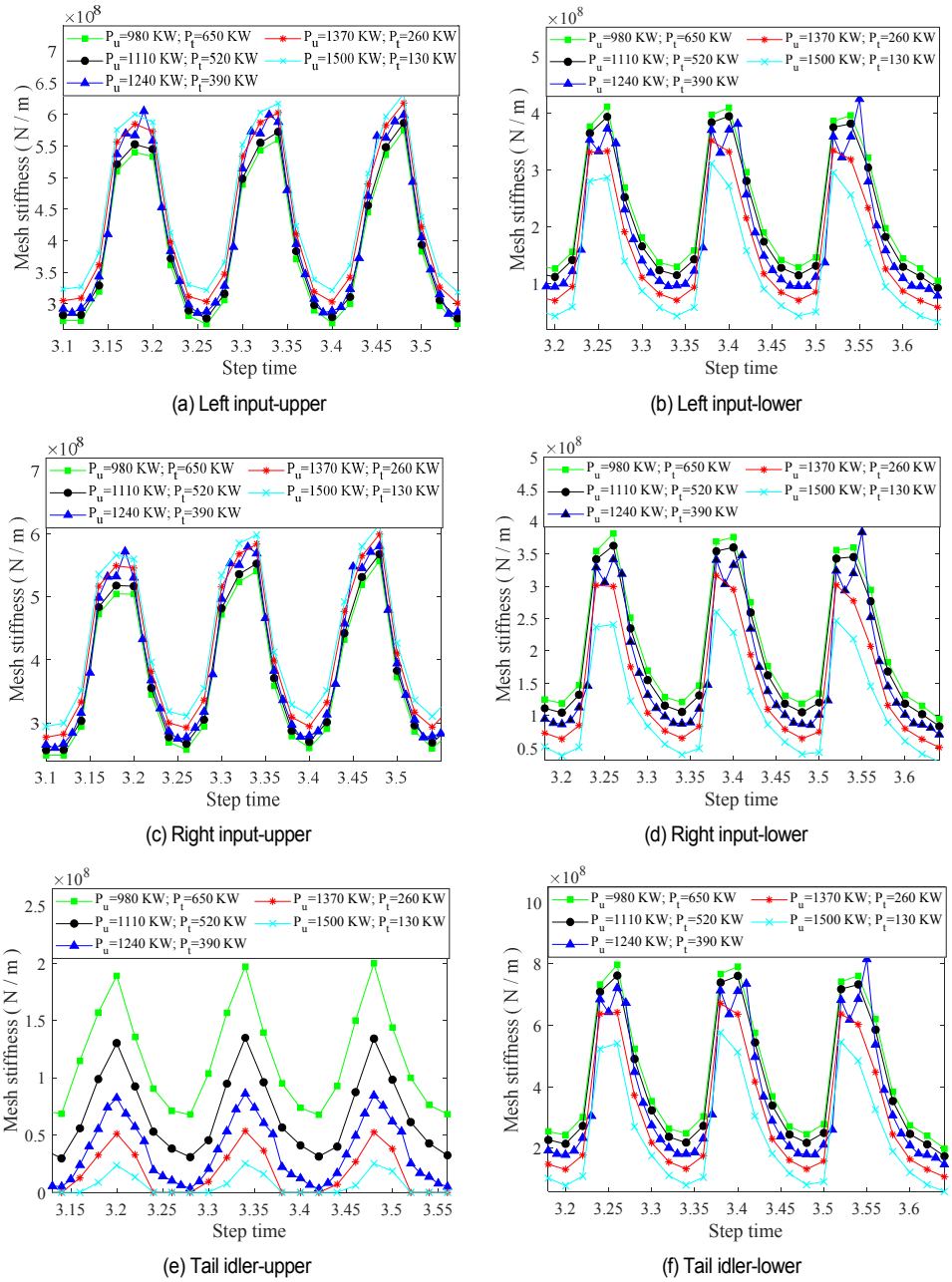

(a) Left input-upper

(b) Left input-lower

(c) Right input-upper

(d) Right input-lower

(e) Tail idler-upper

(f) Tail idler-lower

Fig. 14. TVMS in CFGSTTS with different load distributions.

4.5×10^8 N/m, 0.9×10^8 N/m and 9.8×10^8 N/m. Apparently, except for the gear pair of "tail idler-upper", the mesh stiffness of the other gear pairs in CFGSTTS increases as overall load grows. In addition, the step time of first wave crests in Fig. 13 is 3.18, 3.26, 3.18, 3.26, 3.2 and 3.12 respectively, which is the same for different load conditions.

On one hand, with the increase of overall load, the mesh stiffness grows synchronously, but the phase characteristics of mesh stiffness is not changed. On the other hand, the particularity of power exchange between upper face gear and tail idler is reflected in the fact that as overall load increases, the mesh stiffness of gear pair "tail idler-upper" does not change significantly. In other words, when the ratio of power between upper face gear and tail idler is unchanged, the power transfer between them is largely unaffected. In short, changing the overall load proportionally has little impact on the consistency of mesh stiffness of gear pairs.

Additionally, the power distribution between upper face gear and tail idler may also have a great impact on mesh stiffness. A comparative study is conducted according to parameters in Table 6, where the overall input power P is constant at 1630 KW. Regardless of transmission efficiency, the sum of the power of tail idler and upper face gear is also equal to 1630 KW.

As above, the comparison of mesh stiffness of different power distribution modes under constant overall power is calculated by employing SAM, as demonstrated in Fig. 14.

According to the results in Fig. 14, when the power of tail idler P_t is equal to 650 KW, the maximum mesh stiffness of the gear pairs composed of left and right inputs by meshing with upper face gear respectively reaches 5.4×10^8 N/m, 5.3×10^8 N/m and 2.0×10^8 N/m. Meanwhile, the maximum mesh stiffness of the gear pairs formed by left and right inputs with lower face gear is respectively equal to 4.0×10^8 N/m, 3.8×10^8 N/m and 7.9×10^8 N/m.

When the load power of tail idler P_t is 130 KW, the maximum mesh stiffness of the gear pairs composed of left and right inputs by meshing with upper face gear respectively reaches 6.0×10^8 N/m, 6.0×10^8 N/m and 0.3×10^8 N/m. Meanwhile, the maximum mesh stiffness of the gear pairs formed by left and right inputs with lower face gear is respectively equal to 3.0×10^8 N/m, 3.0×10^8 N/m and 5.5×10^8 N/m. By comparison, when the tail idler's power P_t is equal to 650 KW, the mesh stiffness of six gear pairs is the best in numerical consistency.

Overall, the power distribution between tail idler and upper face gear also has a great impact on the mesh stiffness of gear pairs in CFGSTTS. Specifically, power distribution only changes the value of mesh stiffness of gear pairs without affecting its phase. If the total power of the system is constant, as the load power of tail idler increases, the mesh stiffness of two gear pairs composed of input gears and upper face gear will decrease, while the stiffness of other gear pairs will increase. Therefore, on the premise of constant total power, increasing the load ratio of tail idler is beneficial to improving the vibration and noise of the system.

5. Conclusions

For the purpose of researching the stiffness characteristics of CFGSTTS, a new method of SAM which is suitable for calculating TVMS of closed-loop gear systems with multiple branches is proposed and verified. Based on the application of this method, the influence rules of parameters in CFGSTTS on mesh stiffness are investigated and the following conclusions are drawn.

(i) The mesh stiffness of a gear pair in closed-loop system is quite different from that of an independent gear pair under the same load condition. The mesh stiffness of gear pairs in CFGSTTS is time-varying, and there are differences in numerical value and phase. The difference in numerical value is caused by different load torques of gear pairs. The phase difference is determined by the shaft angles of pinions and the tooth number of a pinion.

(ii) Without considering the flexibility of shafts, hubs and other components, changing the position of pinions on the circumference of face gear has no obvious influence on the mesh stiffness of gear pairs in CFGSTTS.

(iii) The mesh stiffness of gear pairs in CFGSTTS is greatly affected by the overall load. When the load power of face gear and tail idler increases proportionally and synchronously, the stiffness change of gear pair "tail idler-upper" is not obvious, but the mesh stiffness of other gear pairs raises synchronously. It is noticeable, however, that this alteration basically does not reduce the difference of mesh stiffness of gear pairs.

(iv) If the total load power of upper face gear and tail idler is constant, appropriate increase of the load on tail idler results in the decrease of TVMS of two gear pairs composed of input gears and upper face gear as well as the increase of TVMS of other gear pairs. This is conducive to improving the consistency of mesh stiffness of gear pairs in CFGSTTS.

Acknowledgments

The authors gratefully acknowledge the support of the National Key Research and Development Program of China through grant No. 2017YFB1300702. The authors gratefully acknowledge the support of the National Natural Science Foundation of China (NSFC) through grants No.51535012, U1604255, and the support of the Key Research and Development Project of Hunan province through grant No. 2016JC2001.

References

[1] P. Marques, R. Martins and J. Seabra, Analytical load sharing and mesh stiffness model for spur/helical and internal/external gears-Towards constant mesh stiffness gear design, *Mechanism and Machine Theory*, 113 (2017) 126-140.

[2] C. G. Cooley, C. Liu, X. Dai and R. G. Parker, Gear tooth mesh stiffness: A comparison of calculation approaches, *Mechanism and Machine Theory*, 105 (2016) 540-553.

[3] Y. Guo and R. G. Parker, Analytical determination of back-side contact gear mesh stiffness, *Mechanism and Machine Theory*, 78 (2014) 263-271.
[4] C. Xie, L. Hua, J. Lan, X. Han, X. Wan and X. Xiong, Improved analytical models for mesh stiffness and load sharing ratio of spur gears considering structure coupling effect, *Mechanical Systems and Signal Processing*, 111 (2018) 331-347.
[5] N. L. Pedersen and M. F. Jørgensen, On gear tooth stiffness evaluation, *Computers and Structures*, 135 (2014) 109-117.
[6] L. Chang, G. Liu and L. Wu, A robust model for determining the mesh stiffness of cylindrical gears, *Mechanism and Machine Theory*, 87 (2015) 93-114.
[7] J. Zhan, M. Fard and R. Jazar, A CAD-FEM-QSA integration technique for determining the time-varying meshing stiffness of gear pairs, *Measurement*, 100 (2017) 139-149.
[8] M. B. Sánchez, M. Pleguezuelos and J. I. Pedrero, Approximate equations for the meshing stiffness and the load sharing ratio of spur gears including hertzian effects, *Mechanism and Machine Theory*, 109 (2017) 231-249.
[9] Q. Wang, B. Zhao, Y. Fu, X. Kong and H. Ma, An improved time-varying mesh stiffness model for helical gear pairs considering axial mesh force component, *Mechanical Systems and Signal Processing*, 106 (2018) 413-429.
[10] G. I. Sheveleva, A. E. Volkov and V. I. Medvedev, Algorithms for analysis of meshing and contact of spiral bevel gears, *Mechanism and Machine Theory*, 42 (2007) 198-215.
[11] V. I. Medvedev, A. E. Volkov, M. A. Volosova and O. E. Zubelevich, Mathematical model and algorithm for contact stress analysis of gears with multi-pair contact, *Mechanism and Machine Theory*, 86 (2015) 156-171.
[12] A. F. Rincon, F. Viadero, M. Iglesias, P. García, A. de-Juan and R. Sancibrian, A model for the study of meshing stiffness in spur gear transmissions, *Mechanism and Machine Theory*, 61 (2013) 30-58.
[13] A. Saxena, A. Parey and M. Chouksey, Time varying mesh stiffness calculation of spur gear pair considering sliding friction and spalling defects, *Engineering Failure Analysis*, 70 (2016) 200-211.
[14] L. Cui, H. Zhai and F. Zhang, Research on the meshing stiffness and vibration response of cracked gears based on the universal equation of gear profile, *Mechanism and Machine Theory*, 94 (2015) 80-95.
[15] J. G. Verma, S. Kumar and P. K. Kankar, Crack growth modeling in spur gear tooth and its effect on mesh stiffness using extended finite element method, *Engineering Failure Analysis*, 94 (2018) 109-120.
[16] Q. Wang, K. Chen, B. Zhao, H. Ma and X. Kong, An analytical-finite-element method for calculating mesh stiffness of spur gear pairs with complicated foundation and crack, *Engineering Failure Analysis*, 94 (2018) 339-353.
[17] Z. Chen, W. Zhai, Y. Shao, K. Wang and G. Sun, Analytical model for mesh stiffness calculation of spur gear pair with non-uniformly distributed tooth root crack, *Engineering Failure Analysis*, 66 (2016) 502-514.
[18] Y. Luo, N. Baddour and M. Liang, A shape-independent approach to modelling gear tooth spalls for time varying mesh stiffness evaluation of a spur gear pair, *Mechanical Systems and Signal Processing*, 120 (2019) 836-852.
[19] Y. Luo, N. Baddour, G. Han, F. Jiang and M. Liang, Evaluation of the time-varying mesh stiffness for gears with tooth spalls with curved-bottom features, *Engineering Failure Analysis*, 92 (2018) 430-442.
[20] H. Ma, X. Pang, R. Feng, J. Zeng and B. Wen, Improved time-varying mesh stiffness model of cracked spur gears, *Engineering Failure Analysis*, 55 (2015) 271-287.
[21] O. D. Mohammed, M. Rantatalo and J. Aidanpää, Improving mesh stiffness calculation of cracked gears for the purpose of vibration-based fault analysis, *Engineering Failure Analysis*, 34 (SI) (2013) 235-251.
[22] N. K. Raghuwanshi and A. Parey, Experimental measurement of spur gear mesh stiffness using digital image correlation technique, *Measurement*, 111 (2017) 93-104.
[23] J. Dong, J. Tang and Z. Hu, Investigation of assembly, power direction and load sharing in concentric face gear split-torque transmission system, *Meccanica*, 54 (14) (2019) 2485-2506.
[24] F. L. Litvin, A. Fuentes, Q. Fan and R. F. Handschuh, Computerized design, simulation of meshing, and contact and stress analysis of face-milled formate generated spiral bevel gears, *Mechanism and Machine Theory*, 37 (5) (2002) 441-459.
[25] F. L. Litvin, I. G. Perez, A. Fuentes, D. Vecchiato, B. D. Hansen and D. Binney, Design, generation and stress analysis of face-gear drive with helical pinion, *Computer Methods in Applied Mechanics and Engineering*, 194 (36-38) (2005) 3870-3901.
[26] F. L. Litvin, D. Vecchiato, E. Gurovich, A. Fuentes, I. G. Perez, K. Hayasaka and K. Yukishima, Computerized developments in design, generation, simulation of meshing, and stress analysis of gear drives, *Meccanica*, 40 (3) (2005) 291-324.
[27] F. L. Litvin, A. Nava, Q. Fan and A. Fuentes, New geometry of face worm gear drives with conical and cylindrical worms: generation, simulation of meshing, and stress analysis, *Computer Methods in Applied Mechanics and Engineering*, 191 (27-28) (2002) 3035-3054.
[28] F. L. Litvin, *Gear Geometry and Applied Theory*, 1th Ed., PTR Prentice Hall, Englevood Cliffs, USA (1994).
[29] *ISO Standard 6336-1:2006*, Calculation of Load Capacity of Spur and Helical Gears-Part 1: Basic Principles, Introduction and General Influence Factors, International Organization for Standardization, Geneva, Switzerland (2006).

Jianxiong Dong received his M.S. in School of Mechanical and Electrical Engineering at Central South University, China in 2015. He received his B.S. in School of Mechanical and Electrical Engineering at Central South University, China in 2012. He is an Ph.D. candidate in Central South University. His research interests include dynamic, vibration, tooth contact analysis, finite element analysis in gear systems.

Jinyuan Tang is a Professor in School of Mechanical and Electrical Engineering and State Key Laboratory of High Performance Complex Manufacturing of Central South University, Changsha, PR China. His research includes dynamics, design and manufacturing of the gears including face gear and bevel gear, the tooth surface strengthening and gear modification, and machine design.

Zehua Hu received his Ph.D. in School of Mechanical and Electrical Engineering at Central South University, China in 2019. He received his M.S. in School of Mechanical and Electrical Engineering at Central South University, China in 2014. His research interests include gear dynamic, vibration, gear design.